IL NUOVO CIMENTO Vol. 36 C, N. 2 Marzo-Aprile 2013
DOI 10.1393/ncc/i2013-11509-3

Colloquia: Nanoforum 2012

Synthesis and characterization of TiO_2 nanotubes as anodic material in lithium-ion batteries

A. Dell'Era(1), F. Mura(2)(*), M. Pasquali(2), A. Pozio(3) and F. Zaza(3)

(1) *CIRPS - Via Eudossiana 18, 00184 Roma, Italy*
(2) *University of Rome Sapienza - Via del Castro Laurenziano 7, 00161 Rome, Italy*
(3) *ENEA-Casaccia R.C. - Via Anguillarese 301, 00123 S. Maria di Galeria (RM), Italy*

ricevuto il 17 Marzo 2013

Summary. — The aim of this work is to analyze the efficiency of titania nanotubes acting as anode for lithium-ion batteries. The titania nanotubes has been obtained using an anodization process in a ethylene glycol solution, containing ammonium fluoride and a small quantity of water. After a heat treatment, needed to crystallize the material in the anatase form, the nanotubes has been analyzed in their performance as anode in a Li-ion battery. Structural and morphologic characterization of the titania nanotubes have been studied using XRD and SEM analysis, while the galvanostatic cycles has been collected in order to examine the electrochemical performance as electrodic material. Finally, a comparison of the electrochemical performance between our samples and commercial nanostructured titanium oxide, has been made, obtaining that the TiO_2 nanotube electrodes treatmen reduces the overall cell voltage and provides good retention capacity on cycling and higher capacity at all used C-rate.

PACS 82.47.Aa – Battery Lithium-Ion.
PACS 81.97.De – Fabrication composite material.
PACS 82.80.Fk – Electrochemical analysis.

1. – Introduction

In the future, nanomaterials will become more and more important for many industrial and technological applications like photovoltaics, electrochemical energy storage systems, catalytic devices and sensors. Obviously, one of the most important request from the industrial world for a quick development and commercialization of these nanomaterials is a simple and easy to replicate chemical preparation is fundamental. From this point of view, the work of Gong *et al.* [1] has represented a turning point for the titania

(*) E-mail: francesco.mura@uniroma1.it

nanotubes, because this new synthesis permits to obtain these nanostructures through a simple anodic oxidation of a titanium foil in fluoride-based solutions, overtaking previous complex techniques like the sol-gel transcription [2] or the hydrothermal process [3], but at the same time, opening the way to a new methodology able to combine a simplicity of preparation of the material with a complete control of physical characteristics of the nanosystem, such as morphology [4, 5], length and pore size [6], and wall thickness [7]. These features has been obtained by varying the three main parameters of the process: 1) the applied voltage [8, 9]; 2) the anodization time [10, 11]; 3) the components and concentration of the electrolyte solutions [12, 13]. The model of the nanotube array formation has been exposed by Grimes *et al.* [14], and basically consists in a competition between the chemical dissolution of the titanium dioxide by the acting of the fluoride, according the reaction $TiO_2 + 6F^- + 4H^+ \rightarrow TiF_6^{2-} + 2H_2O$, and the oxide growth at the metal/oxide interface due to the presence of a small quantity of water in the anodization bath. One of the most researched activities concerning this titania nanotubes is the application as photo-anode in water-photoelectrolysis, which have proved that these nanosystems [10, 15] provide elevated efficiency values of UV photoconversion. In the meanwhile, a large range of different applications for this nanomaterial has been experimented. In fact, it is reported that the electrical resistance of the titania nanotubes was highly dependent to the chemisorbed hydrogen molecules [16, 17], creating a new route in the hydrogen sensing research field [18, 19], while other similar examples of the wide versatility in many different areas of the TiO_2 nanotube arrays are available in literature, from the dye-sensitized solar cells [20-23] to many biological and medical research fields, as the osteoblast growth [24-27] or drug elution [28-31]. Instead, in this work we want to analyze the behavior of this material working as anode for lithium-ion batteries [32], because, Li-ion batteries are tempting power devices due to their high energy density. The successful electrochemical and chemical insertion of lithium into titanium dioxides has already been demonstrated [33, 34]. TiO_2 has various polymorphs, such as anatase, rutile, brookite or TiO_2 (B), but the lithium insertion has been given satisfactory results only for anatase [34-37] and TiO_2 (B) [38, 39]. Besides, TiO_2 anatase has been demonstrated to be a promising electrode material for Li-ion batteries due to its good Li-storage capacity (335 $mAhg^{-1}$ corresponding to the insertion of one Li per TiO_2 inducing a complete reduction $Ti^{4+} \rightarrow Ti^{3+}$), cycling stability and safety against overcharging [36]. In addition, it is a non-toxic, cheap material The structure of the mesoporous nanotubes was specifically designed to allow efficient transport of both lithium ions and electrons, which are necessary for a high rate rechargeable battery [40]. From a practical viewpoint, reversible insertion of Li into anatase is about 0.6 (*i.e.* 200 $mAhg^{-1}$) at 1.78 V *versus* Li^+/Li [35, 36]. But its electrochemical performance strongly depends on the size and shape of particles [36, 41, 42]. In this article we analyze the good behavior of titania nanotubes, grown by anodization process in glycol ethylene solution, acting as electrode for lithium batteries.

2. – Experimental

2˙1. *Synthesis of titania nanotube arrays.* – Thin sheets of commercially pure grade-3 titanium (Titania, Italy) have been used as substrate for the nanotube growth. The samples have dimensions of 55 mm × 15 mm with a thickness of 0.5 mm, and were arranged to show an active area of 1 cm^2. After 3 min of pickling in a solution made dissolving HF (Carlo Erba) / HNO_3 (Carlo Erba) (volumetric ratio of 1:3) in deionised water up to a final volume of to 100 ml, all the titanium sheets have been placed in a three-electrode cell

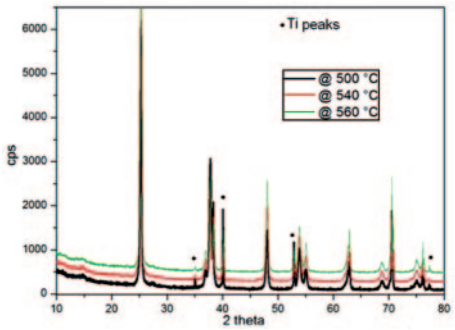

Fig. 1. – Comparison of XRD patterns of the samples at different temperature. Each peak attributed to TiO_2 anatase phase is indicated with an asterisk.

containing a 1 M KOH solution (Carlo Erba) and subjected to a prefixed and optimized density current (1 mA/cm^2) generated by a potentiostat/galvanostat (Solartron 1286) for 3 min, so to generate a fixed oxide layer [43]. The counter-electrode is a platinum sheet, while the reference is a standard calomel electrode (SCE). The growth of the nanotube arrays has been operated in the system described in our previous work [43], using a glycol ethylene solution with 1 %wt. H_2O and 0.20 %wt. NH_4F for 3 h at 60 V. After the anodization, all the samples were washed in glycol ethylene and left overnight in a dry room. In order to transform amorphous TiO_2 nanotubes obtained by anodic growth into the crystalline phase of the anatase, all the samples have been placed in a tubular furnace (Lenton) for 1 h in air, at different temperatures, using a slope of 1 °C/min.

2˙2. *Characterization of titania nanotube arrays.* – The samples crystallized at 500, 540 and 580 °C, respectively, are characterized performing XRD analysis in order to identify the crystalline structure of TiO_2 nanotubes. The results confirmed the presence of the anatase, together with other crystalline phases. All samples give XRD diffraction patterns having both the peaks related to the Ti support and the peaks related to TiO_2 anatase phase, observed at 35°, 40°, 57° and 77°.

Looking at fig. 1, the anatase phase formation starts at 500 °C, while the increasing of the temperature causes the decrease of the peaks related to metallic Ti while increases the ones of the titania because of the transition from amorphous to crystalline structure of TiO_2 covering layer. The presence of TiO_2 rutile phase is not observed, because the characteristic peak at 23° is absent. Despite the diverse temperature treatments, any difference in crystalline structure and chemical composition of the prepared nanostructured titanium oxides has been observed. From the FESEM images it is possible to obtain the TiO_2 nanotube geometric parameters such as the average length and the average external and internal diameters, that are around 20 nm (fig. 2a), 200 nm (fig. 2b) and 100 nm (fig. 2c), respectively. The nanotube surface is smooth, but it is not shiny (fig. 2d).

2˙3. *Synthesis and characterization of titania-nanotube–based anodes.* – A powder, containing the titania nanotubes, is obtained scratching the surface of the sheet and grinded into an agate mortar, in order to obtain their breaking up without causing an excessive trituration, together with the binder and the electronic conductive material for preparing the electrode for lithium batteries. The composite material has the following composition: powder containing titania nanotubes 60% wt., Teflon 15% wt. and SuperP

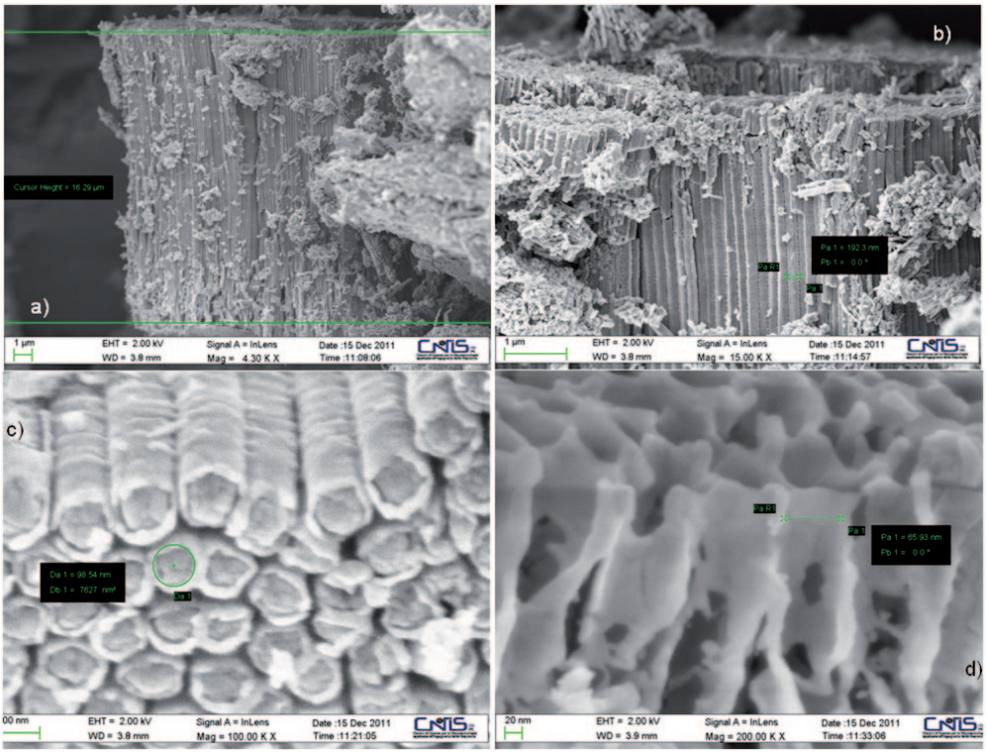

Fig. 2. – FESEM images of TiO_2 nanotubes at various magnifications: a) 4.3 kX, b) 15 kX, c) 100 kX, d) 200 kX.

carbon black 25% wt. respectively. This solid mixture undergoes a calendering processes which produces a tape, from which the disk-shape anode is acquired. Figure 3 shows the top-view FESEM images of the surface of the obtained anode, that is composed of fragmented single and agglomerated nanotubes, homogeneously mixed with Teflon and SuperP carbon black.

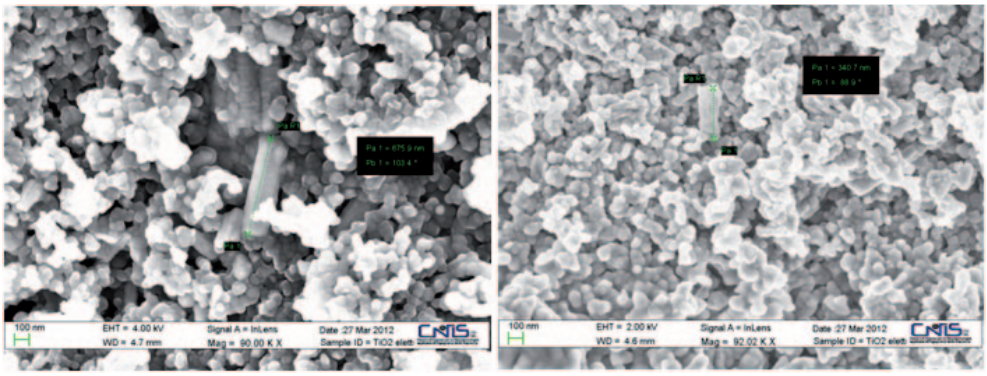

Fig. 3. – FESEM images of TiO_2-nanotubes–based anode.

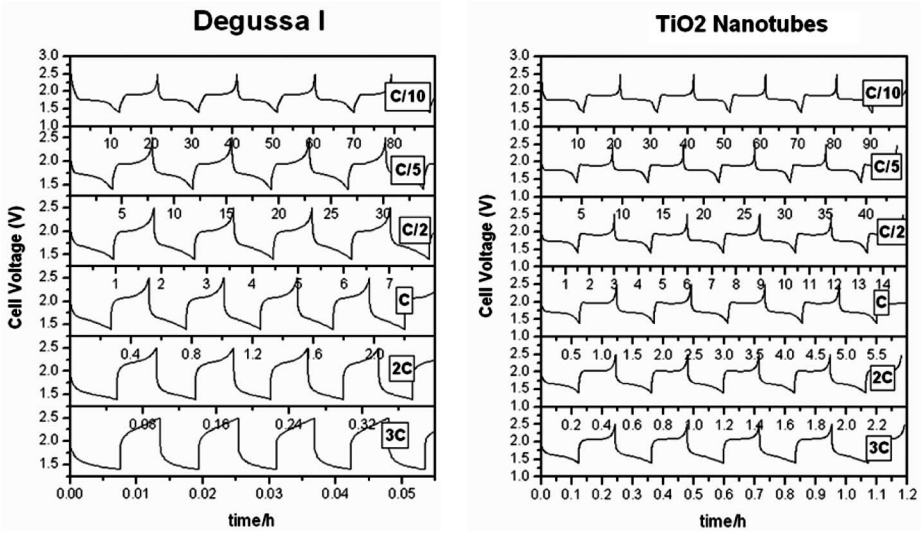

Fig. 4. – Cell voltage *vs.* time/h for different galvanostatic cyclings for TiO_2-nanotube–based anode and P-25.

The electrochemical measurements are performed on the sample sintered at 580 °C and compared with the commercial nanostructured titanium oxide P-25 (Degussa). T-shaped cells are assembled as follows: working cathode (TiO_2, Teflon, carbon) / electrolyte ($LiPF_6$EC:DMC 1/1)/anode(lithium). Galvanostatic cycling experiments on T-shaped cells were performed at various charge/discharge rates. The experimental procedure was based on the following protocol: 1) five cycles of charge and discharge at C/10 rate; 2) five cycles of charge and discharge at C/5 rate; 3) five cycles of charge and discharge at C/2; 4) five cycles of charge and discharge at C rate; 5) five cycles of charge and discharge at 2C rate; 6) five cycles of charge and discharge at 3C rate. The results of the experiments are showed in fig. 4 (cell voltage *vs.* time) and 5 (cell voltage *vs.* specific capacity), for each charge/discharge rate.

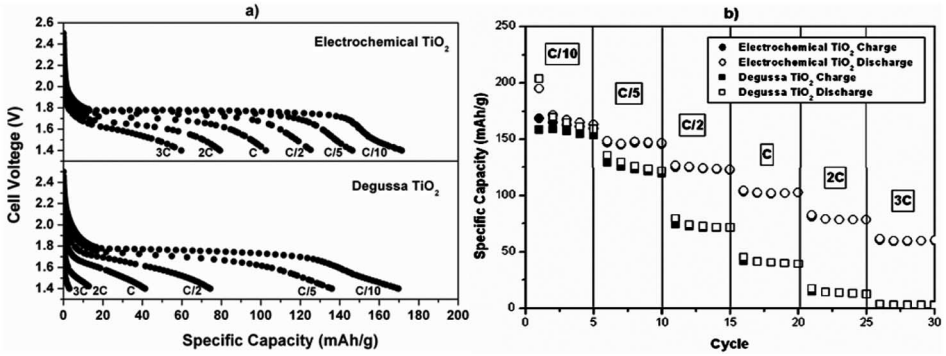

Fig. 5. – Galvanostatic cycling at C/10, C/5, C/2, C, 2C and 3C: a) cell voltages against specific capacity; b) specific capacity against cycle number.

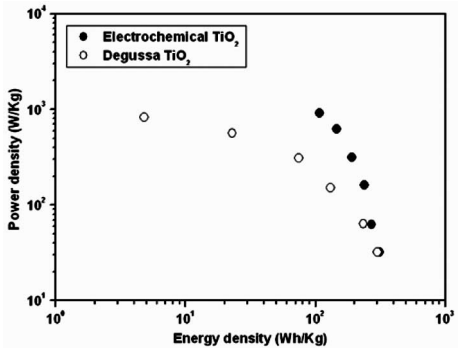

Fig. 6. – Ragone Plot (power density/WKg^{-1} *vs.* energy density/$WhKg^{-1}$) for titania-nanotubes–based anode (○) and commercial TiO_2 (●).

Figure 4 demonstrates the improved performance of the cell using the electrode containing the fragmented titania nanotubes, respect to the commercial titania powder for the flatter shapes of the charge/discharge curves, also at high C rate. The better performances of TiO_2 nanotubes rather than TiO_2 nanopowder are more evident in fig. 5a, where the cell voltages are plotted against the specific capacity. In fact, from this graph, it can be observed that this kind of electrodes allows full reversible intercalation/de-intercalation processes, promoting high specific capacity also at high C rates (fig. 5b). The difference in specific capacity at C/10 rate is minima even if the value 165 mAh/g for TiO_2 nanotubes is almost the same of the theoretical value (0.168 mAh/g). The difference between the specific capacity of TiO_2 nanotubes and TiO_2 nanopowder becomes significant with the charge/discharge rate increases. In particular, at 3C rate the specific capacity of TiO_2 nanopowder is almost zero, while the specific capacity of TiO_2 nanotubes is around 70 mAh/g. In addition, TiO_2 nanotubes do not undergo any capacity loss at every cycling rate, also at 3C rate, while TiO_2 nanopowder undergoes a significant capacity loss at low rate, such as C/5. Finally, the Ragone plot (fig. 6) [44], in which the vertical axis describes how much energy is available, while the horizontal axis shows the power per unit mass, gives another proof of the improved performance for our composite electrode showing that it is possible to obtain the highest specific energy at the same specific power.

3. – Conclusion

Titania nanotubes have been synthesized by the electrochemical anodization technique, sintered in the anatase crystalline phase and mixed together with carbon super S and teflon, so to obtain the composite material that forms our anode. The electrochemical performance in cells have showed a good reversibility of the electrode material, providing a capacity of 165 mAh/g at C/10 and 70 mAh/g at 3C. Comparing the electrochemical performances of TiO_2 nanotubes and commercial nanostructured TiO_2 (Degussa P25) showed how the nanotubic morphology allows to obtain higher capacity. The best performance of TiO_2 nanotubes are highly significant at high currents density. In fact, Ragone plot shows that the energy density of TiO_2 nanotubes and commercial TiO_2 are 100 Wh/kg and 40 Wh/kg, respectively, at 1000 W/kg power density. We can therefore conclude that the TiO_2 nanotubes are suitable to replace the graphite in lithium-ion batteries for power applications.

REFERENCES

[1] Gong D., Grimes C. A., Varghese O. K., Hu W., Singh R. S., Chen Z. and Dickey E. C., *J. Mater. Res.*, **16** (2001) 3331.
[2] Hoyer P., *Langmuir*, **12** (1996) 1411.
[3] Kasuga T., Hiramatsu M., Hoson A., Sekino T. and Niihara K., *Langmuir*, **14** (1998) 3160.
[4] Mor G. K., Varghese O. K., Paulose M., Mukherjee N. and Grimes C. A., *J. Mater. Res.*, **18** (2003) 2588.
[5] Kontos G. K., Kontos A. I., Tsoulkleris D. S., Likodimos V., Kunze J., Schmuki P. and Falaras P., *Nanotechnology*, **20** (2009) 045603.
[6] Cai Q., Paulose M., Varghese O. K. and Grimes C. A., *J. Mater. Res.*, **20** (2005) 230.
[7] Mor G. K., Shankar K., Paulose M., Varghese O. K. and Grimes C. A., *Nano Lett.*, **5** (2005) 191.
[8] Wang J. and Lin Z., *J. Phys. Chem. C*, **113** (2009) 4026.
[9] Su Z. and Zhou W., *J. Mater. Chem.*, **19** (2009) 2301.
[10] Shankar K., Mor G. K., Prakasam H. E., Yoriya S., Paulose M., Varghese O. K. and Grimes C. A., *Nanotechnology*, **18** (2007) 065707.
[11] Macak J. M., Hildebrand H., Marten-Jahns U. and Schmuki P., *J. Electroanal. Chem.*, **621** (2008) 254.
[12] Kim H. and Lee K., *Electrochem. Solid-State Lett.*, **12** (2009) C10.
[13] Fahim N. F., Sekino T., Morks M. F. and Kusunose T., *J. Nanosci. Nanotechnol.*, **9** (2009) 1803.
[14] Grimes C. A., Varghese O. K. and Ranjan S., *The Solar Hydrogen Generation By Water Photoelectrolysis* (Springer) 2008.
[15] Mura F., Masci A., Pasquali M. and Pozio A., *Electrochim. Acta*, **55** (2010) 2256.
[16] Varghese O. K., Gong D., Paulose M., Ong K. G., Dickey E. C. and Grimes C. A., *Adv. Mater.*, **13** (2003) 624.
[17] Varghese O. K., Gong D., Paulose M., Ong K. G. and Grimes C. A., *Sens. Actuators B*, **93** (2003) 338.
[18] Chen Q., Xu D., Wu Z. and Liu Z., *Nanotechnology*, **19** (2008) 365708.
[19] Sennik E., Colak Z., Kilinc N. and Ozturk Z. Z., *Int. J. Hydrogen Energy*, **35** (2010) 4420.
[20] Mor G. K., Shankar K., Paulose M., Varghese O. K. and Grimes C. A., *Appl. Phys. Lett.*, **91** (2007) 152111.
[21] Mor G. K., Basham J., Shankar K., Paulose M., Kim S., Varghese O. K., Vaish A., Yoriya S. and Grimes C. A., *Nano Lett.*, **10** (2010) 2387.
[22] Wang Y., Yanh H., Liu Y., Wang H., Shen H., Yan J. and Xu H., *Progr. Photovoltaics: Res. Appl.*, **18** (2010) 285.
[23] Alivov Y. and Fan Z. Y., *J. Mater. Sci.*, **45** (2010) 2902.
[24] Liu Z. and Misra M., *Nanotechnology*, **21** (2010) 125703.
[25] Os S. H., Finones R. R., Daraio C., Chen L. H. and Jin S., *Biomaterials*, **26** (2005) 4938.
[26] Os S. H. and Jin S., *Mater. Sci. Eng. C*, **26** (2006) 1301.
[27] Os H. J., Lee J. H., Kim Y. J., Suh S. J., Lee J. H. and Chi C. S., *Mater. Chem. Phys.*, **109** (2008) 10.
[28] Das K., Bandyopadhyaya A. and Bose S., *J. Am. Chem. Soc.*, **91** (2008) 2808.
[29] Popat K. C., Eltgroth M., Latempa T. J., Grimes C. A. and Desai T. A., *Biomaterials*, **28** (2007) 4880.
[30] Popat K. C., Eltgroth M., Latempa T. J., Grimes C. A. and Desai T. A., *Small*, **11** (2007) 1878.
[31] Peng L., Mendelsohn A. D., Latempa T. J., Yoriya S., Grimes C. A. and Desai T. A., *Nano Lett.*, **9** (2009) 1932.

[32] Fang D., Liu S. O., Chen R. Y., Huang K. L., Li J. S., Yu C., Qin D. Y. and Xuebao W. C., *J. Inorg. Mater.*, **23** (2008) 647.
[33] Murphy D., Cava R., Zahurak S. and Santoro A., *Solid State Ionics*, **9–10** (1983) 413.
[34] Zachau-Christiansen B., West K., Jacobsen T. and Atlung S., *Solid State Ionics*, **28–30** (1998) 1176.
[35] Ohzuku T., Kodoma T. and Hirai T., *J. Power Sources*, **46** (1985) 1176.
[36] Huang S., Kavan L., Exnar I. and Gratzel M., *J. Electrochem. Soc.*, **142** (1995) L142.
[37] Kavan L., Gratzel M., Rathousky J. and Zukal A., *J. Electrochem. Soc.*, **143** (1996) 394.
[38] Armstrong G., Armstrong R., Canales J., Garcia R. and Bruce P., *Adv. Mater.*, **17** (2005) 862.
[39] Armstrong G., Armstrong R., Canales J., Garcia R., Bruce P., Reale P. and Scrosati B., *Adv. Mater.*, **18** (2006) 2597.
[40] Wang K., Wei M., Morris M. A., Zhou H. and Holmes J. D., *Adv. Mater.*, **19** (2007) 3016.
[41] Kavan L., Attia A., Lenzmann F., Elder S. and Gratzel M., *J. Electrochem. Soc.*, **147** (2000) 2897.
[42] Kavan L., Rathousky J., Gratzel M., Shklover V. and Zukal A., *J. Phys. Chem. B*, **104** (2000) 12012.
[43] Mura F., Pozio A., Masci M. and M. P., *Electrochim. Acta*, **54** (2009) 3794.
[44] Ragone D., *SAE Technical Paper* (1968).